ISSN 2176-5480

22nd International Congress of Mechanical Engineering (COBEM 2013)
November 3-7, 2013, Ribeirão Preto, SP, Brazil


# A COMPUTER PROGRAM FOR CALCULATING NORMAL AND OBLIQUE SHOCK WAVES FOR AIRFLOWS IN CHEMICAL AND THERMODYNAMIC EQUILIBRIUM

**Augusto Fontan Moura**
**Maurício Antoniazzi Pinheiro Rosa**
Instituto de Estudos Avançados, São José dos Campos, SP, Brasil
augustofontan@gmail.com
pinheiro@ieav.cta.br

***Abstract.*** *This work presents the modeling and validation results of a newly developed computer program for calculating airflow conditions behind normal and oblique shock waves considering two distinct gas models for the air: a) calorically perfect and b) chemical and thermodynamic equilibrium. In the latter, high temperature effects in the air such as molecular vibration and dissociation and atomic ionization are taken into account by using the mathematical correlations for the air properties given by Srinivasan and Tannehill. By yielding pressure, temperature and Mach number of the air free stream, it is possible to obtain the results for the airflow conditions behind a normal and/or oblique shock wave. The program can also calculate oblique shock waves generated by a sequence of compression ramps such as in scramjet intakes, for instance, by yielding sequences of ramp angles. Besides the models and methodology used for developing the computer program, this work also presents some results of model validation and code verification as well as an analysis of high temperature effects on the airflow in scramjet intakes operating at different conditions.*

***Keywords:*** *computer program, chemical equilibrium air, normal shock, oblique shocks, scramjet*

## 1. INTRODUCTION

The analysis of high speed airflows involves, in general, very high temperatures. It is known that by raising the temperature of the air above a certain value, molecular vibrational mode starts becoming important. By further increasing the air temperature, molecular dissociation as well as recombination reactions may also occur. For even higher temperatures, the process of atomic ionization may also take place. Each one of these processes has some impact on the properties of the air. For instance, for air at sea level conditions, the $O_2$ and $N_2$ molecular vibrational energies start becoming significant above approximately 800 K, whereas chemical reactions start only at approximately 2500 K with the $O_2$ dissociation, which is accompanied by $N_2$ dissociation (above 4000 K) and several recombination reactions. At considerably higher temperature, approximately 9000 K, all the nitrogen and oxygen molecules have already dissociated and atomic ionization starts taking place so that we have a partially ionized plasma ($O$, $O^+$, $N$, $N^+$ and electrons). All these processes may alter considerably the airflow properties so that the air can no longer be treated simply as calorically perfect gas with the penalty of obtaining very poor results. Also, it is important to mention that by reducing pressure, dissociation and ionization onset temperatures also decrease (Anderson, 1989), so high temperature effects in the air become even more important in high altitude hypersonic flights such as for reentry and scramjet vehicles.

For the researches under development at the Institute for Advanced Studies (IEAv) in hypersonics and aerothermodynamics, calculations including such high temperature effects in the air are constantly required for several flight conditions. So, the need for a simple and user-friendly program, instead of complex CFD codes which can be cumbersome and do more than is actually needed, became an important issue for calculating the properties behind normal and oblique shock waves for chemical and thermodynamic equilibrium air.

Tabulated data is available for chemical and thermodynamic equilibrium air at several conditions and calculations can be performed using different approaches. Here, the one which uses the polynomial curve fittings presented by Tannehill and Mugge (1974) and later improved by Srinivasan *et al.*, 1987, is considered. Such calculations involve large polynomials with tabulated coefficients that vary greatly with the free-stream conditions.

The paper presents the models and methodology used in the program development as well as result comparison with extensive data from the literature in order to verify the program and validate the models. It also presents results for a scramjet intake configuration, obtained for perfect gas and chemical and thermodynamic equilibrium air, assessing the impact of gas modeling on the flow conditions in the scramjet intake.

ISSN 2176-5480



## 2. MODELS AND METHODOLOGY

The program was developed using Fortran 95 programming language, suitable to numeric calculations such as the ones required for the shock relations. For a given free-stream airflow, the program can calculate flow properties behind a normal and/or an oblique shock wave, as well as in a sequence of oblique shock waves for both air gas models: calorically perfect and chemical and thermodynamic equilibrium. For calculations of flows in a sequence of oblique shock waves, the flow deflection angle for each shock wave should also be given. Regardless of the gas model considered, free stream airflow is treated as calorically perfect gas for which Mach number, pressure and temperature are provided. So, the free-stream properties are calculated from Eq. (1). Since the program deals with atmospheric air, values are $\gamma$=1.4 and $R = 287\ [J/kg \cdot K]$. The following calorically perfect and shock relations can be found in Anderson (1990). The perfect gas equation is given by:

$$p = \rho R T \tag{1}$$

where $p$ is the pressure, $T$ is the temperature, $\rho$ is the density and $R$ is the air gas constant. From this equation, density can be obtained from the known values of pressure and temperature.

Specific heats at constant volume, $c_{v,}$ and constant pressure, $c_p$, are calculated from Eq. (2) and Eq. (3), respectively.

$$c_v = {}^{R}\!/_{\gamma} - 1 \tag{2}$$

$$c_p = \gamma c_v = \frac{\gamma R}{\gamma - 1} \tag{3}$$

where γ is the specific heat ratio.

The specific internal energy, $e$, and the enthalpy, $h$, can be obtained by Eq. (4) and (5), respectively.

$$e = c_v T \tag{4}$$

$$h = c_p T = \left(\frac{\gamma R}{\gamma - 1}\right) T \tag{5}$$

The sound speed, $a$, and the free stream velocity, $u$, are obtained, respectively, by Eqs. (6) and (7).

$$a = \sqrt{\gamma R T} \tag{5}$$

$$u = M a \tag{6}$$

Lastly, the stagnation pressure, $p_0$, is calculated by the isentropic relations given by Anderson (1990), as shown in Eq. (8).

$$p_0 = p\left(1 + \frac{\gamma - 1}{2} M^2\right)^{\frac{\gamma}{\gamma - 1}} \tag{7}$$

### 2.1 Normal shock calculation methodologies

Normal shock calculations are needed in many situations in high speed applications such as for the normal shocks generated inside of a shock tube and also in bow shock around a blunt body at a point on the shock wave whose tangent is perpendicular to the supersonic flow (point A in Fig. 1), among many others.

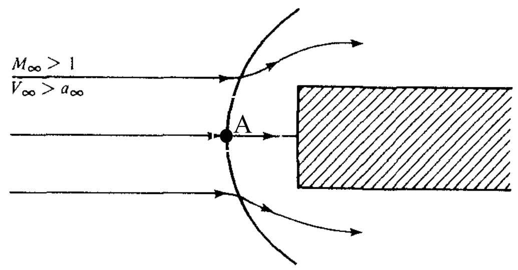


Figure 1 – Schematic showing the bow shock wave- around a blunt body (Anderson,1989) and point A where the normal shock relations stand.

ISSN 2176-5480



Figure 2 shows a schematic of a normal shock and the flow properties ahead and behind the shock The subscript 1 indicates the flow properties ahead of the shock, while 2 indicates conditions behind the shock wave.

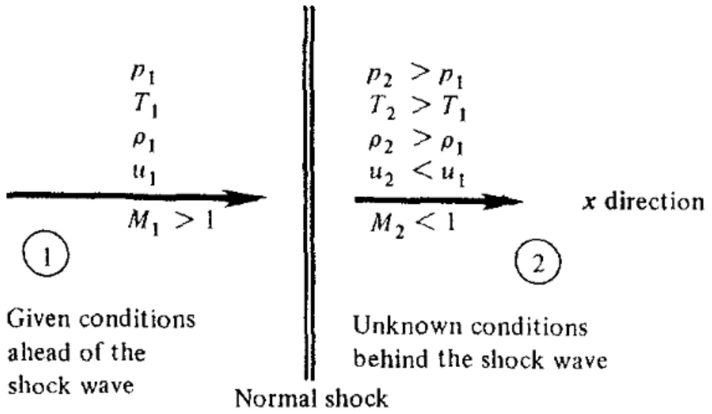


Figure 2 - Schematic of a normal shock and the flow properties ahead and behind of the shocl

.Normal shock calculations are performed by using the one-dimensional form of the continuity, momentum and energy equations as given by Eqs. (9), (10) and (11), respectively (Anderson (1990).

$$\rho_1 u_1 = \rho_2 u_2 \tag{8}$$

$$p_1 + \rho_1 u_1^2 = p_2 + \rho_2 u_2^2 \tag{9}$$

$$h_1 + \frac{u_1^2}{2} = h_2 + \frac{u_2^2}{2} \tag{10}$$

### 2.1.1 Normal shock relations for calorically perfect gas

Assuming air as a calorically perfect gas, Eq. (1) and Eq. (5) for the properties behind the shock, can be added to Eqs. (9) through (11) to form a closed system of five unknown variables ($p_2$, $T_2$, $h_2$, $u_2$, $\rho_2$), which can be solved to obtain the properties behind the shock as a function of free stream Mach number, $M_1$, as presented in Eqs. (12) through (15).

$$\frac{\rho_2}{\rho_1} = \frac{u_1}{u_2} = \frac{(\gamma+1)M_1^2}{2+(\gamma-1)M_1^2} \tag{11}$$

$$\frac{p_2}{p_1} = 1 + \frac{2\gamma}{\gamma+1}(M_1^2 - 1) \tag{12}$$

$$\frac{T_2}{T_1} = \frac{p_2}{p_1}\frac{\rho_1}{\rho_2} = \frac{e_2}{e_1} = \frac{h_2}{h_1} \tag{13}$$

$$M_2^2 = \frac{M_1^2+[2/(\gamma-1)]}{[2\gamma/(\gamma-1)]M_1^2-1} \tag{15}$$

The increase in entropy across the shock, $\Delta s$, is calculated by Eq. (12) obtained from the second law of thermodynamics.

$$\Delta s = c_p \ln\frac{T_2}{T_1} - R\ln\frac{p_2}{p_1} \tag{16}$$

The total pressure behind the shock can be obtained by Eq. (13).

$$\frac{p_{0_2}}{p_{0_1}} = e^{-\Delta s/R} \tag{17}$$

The calculated values behind the shock are all listed in an output file generated by the program, along with the free stream values.

ISSN 2176-5480



### 2.1.2 Normal shock relations for chemical and thermodynamic equilibrium air

In hypersonic flows, high temperatures can be achieved behind the shock waves such that the air no longer behaves as a calorically perfect gas. In these conditions, the specific heats are not constants, ceasing to obey the relations presented in Eq. (4) and Eq. (5); oxygen and nitrogen molecule dissociation, atomic ionization and recombinations may also happen, further complicating the calculations and invalidating the use of the perfect gas equation of state given by Eq. (1). Equations (9), (10) and (11) still hold but the calorically perfect equations, Eqs. (1) through (6), are no longer suitable, so additional equations should be provided in order to close the system for equilibrium air. In this work, these additional equations are polynomial fittings of tabulated data of the thermodynamic properties for chemical and thermodynamic equilibrium air (Srinivasan *et al.,* 1987). The polynomial fitting for pressure as function of internal energy and density, Eq. (18), along with the thermodynamic relation for the internal energy, Eq. (19), for the properties behind the shock, were used to close the system.

$$p_2 = f_p(e_2, \rho_2) \tag{18}$$

$$e_2 = h_2 - \frac{p_2}{\rho_2} \tag{19}$$

The system formed by Eqs. (9), (10),(11), (18) and (19) is solved iteratively for the variables $(p_2, e_2, h_2, u_2, \rho_2)$ by using the secant method with the density, $\rho_2$, as the iterating variable and the pressure, $p_2$, as the dependent variable.

Once the system has been solved, other properties of the flow behind the shock can be calculated using polynomial correlations from Sirinivasan et al, 1987, such as: temperature, $T_2 = f_T(e_2, \rho_2)$, sound speed, $a_2 = f_a(e_2, \rho_2)$, and entropy, $s_2 = f_s(e_2, \rho_2)$.

### 2.2 Oblique shock wave calculations methodology

The oblique shock waves, differently from normal shock waves, are two-dimensional since the flow change direction after passing the shock. Therefore, the free stream velocity has normal and tangential components, $u_1$ and $w_1$, which are, respectively, associated to the components of the Mach number, $M_{n_1}$ and $M_{t_1}$ (Anderson, 1990), as shown in Figure 3. Also, in this figure, the angles $\beta$ and $\theta$ are, respectively, the shock wave and behind shock velocity angles.

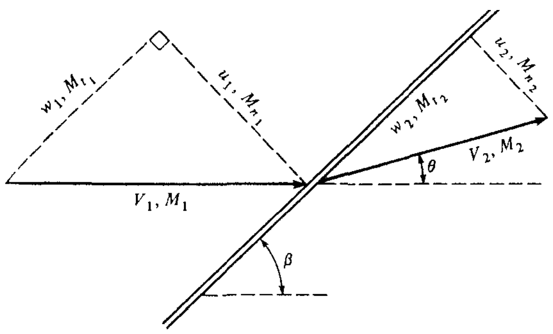


Figure 3 - Oblique shock wave diagram.

However, the set of continuity, momentum and energy equations across the shock, Eqs. (9), (10) and (11), still hold for the oblique shock calculations for the normal component of the income flow, which is the only responsible for the physical and thermal property changes of the flow across the oblique shock. Therefore, calculations of an oblique shock wave are equivalent to the ones of a normal shock considering the normal component of the free stream flow and taken into the account that the tangent components remain unchanged across the shock.

The flow behind an attached oblique shock wave generated by a ramp is always parallel to the ramp, so the schematic in Fig. 2 also represents the case of a the shock wave generated by a $\theta$-angle ramp with respect to the income flow.

The normal components of the free stream Mach number, $M_{n_1}$, and velocity are given by:

$$M_{n_1} = M_1 \sin\beta \ \ or \ u_1 = V_1 \sin\beta \tag{20}$$

Therefore, to calculate the normal components of the free stream, it is necessary to have the shock wave angle, $\beta$, which is not known a priori since what is given as input is the ramp angle $\theta$ and the free stream conditions. The $\beta$-angle is calculated using the trigonometric relation, Eq. (21), obtained from Fig.2.

ISSN 2176-5480



$$\frac{\tan(\beta-\theta)}{\tan\beta} = \frac{u_2}{u_1} \tag{21}$$

The oblique shock wave relations are, therefore, the same as in Eq. (12) to (14), substituting $M_1$ for $M_{n_1}$. The normal component of the Mach number behind the shock wave is given by Eq. (15), again substituting $M_1$ for $M_{n_1}$.

### 2.2.1 Oblique shock wave relations for calorically perfect gas

Considering the air as a calorically perfect gas, all relations given by Eqs. (12) through (17) are also valid for an oblique shock replacing the Mach number, $M$, there by the normal component, $M_n$, given by Eq. (20), for the oblique shock. The wave angle, *β, is* calculated from Eq. (21) by using Eq. (12) and (20) to get, after some manipulation, what is called, the *β-θ-M* relation for calorically perfect gas (Anderson, 1990), given by Eq. (14).

$$\tan\theta = 2\cot\beta\left[\frac{M_1^2\sin^2\beta-1}{M_1^2(\gamma+\cos 2\beta)+2}\right] \tag{22}$$

Considering the parameters $\theta$ and $M_1$ as known in this equation, the resulting equation does not have an analytical solution for *β*. Therefore, again the secant method is used to iteratively calculate *β* and then to calculate the flow variables in Eqs. (12) through (17) by replacing the Mach numbers by their respective normal components for the oblique shock..

The Mach number behind the oblique shock, then is calculated from Eq. (23).

$$M_2 = \frac{M_{n_2}}{\sin(\beta-\theta)} \tag{23}$$

### 2.2.2 Oblique shock wave relations for chemical and thermodynamic equilibrium air

Considering the air in chemical and thermodynamic equilibrium behind an oblique shock wave, the procedure is similar to the one presented in Section 2.2.1 for calorically perfect gas except that the flow properties do not obey the perfect gas equation of state, instead they are given by the Sirinivasan's correlations. Also in Eq. (21), the wave angle *β* is not the only unknown, as for the perfect gas model, since the normal velocity components are not known a priori either. Therefore, the system of equations to be solved consists of Eqs. (9), (10),(11), (18), (19) - for the normal shock calculations whose unknowns are: $(p_2, e_2, h_2, u_2, \rho_2)$ - and also of Eqs. (20) and (21), for the calculations of the wave angle, *β,* and the normal component of the income flow, $u_1$ .

This set of equations is solved again iteratively in two loops: an inner loop, which solves the normal shock (Eqs. (9), (10),(11), (18), (19)), as described in Section 2.1.2, and an outer loop, which solves Eqs. (20) and (21) using also the secant method with *β* as the iterating variable. So, initially guessing a value for *β*, velocity $u_1$ is calculated by Eq. (21), which is used to calculate the normal shock (inner loop), which, by its turn, return a value for the velocity, $u_2$. These normal velocity components are then used to verify the previous value of *β.* This procedure is repeated until convergence is reached for the wave angle. As before, by the end of the overall iterative calculations, additional behind of shock flow properties are calculated such as Mach number (Eq. (23)), temperature, speed of sound and entropy, as already mentioned in Section 2.1.2.

### 2.3 Program flowchart

A simplified flowchart for the program, representing the calculations and iterative processes, is presented in Figure 4.

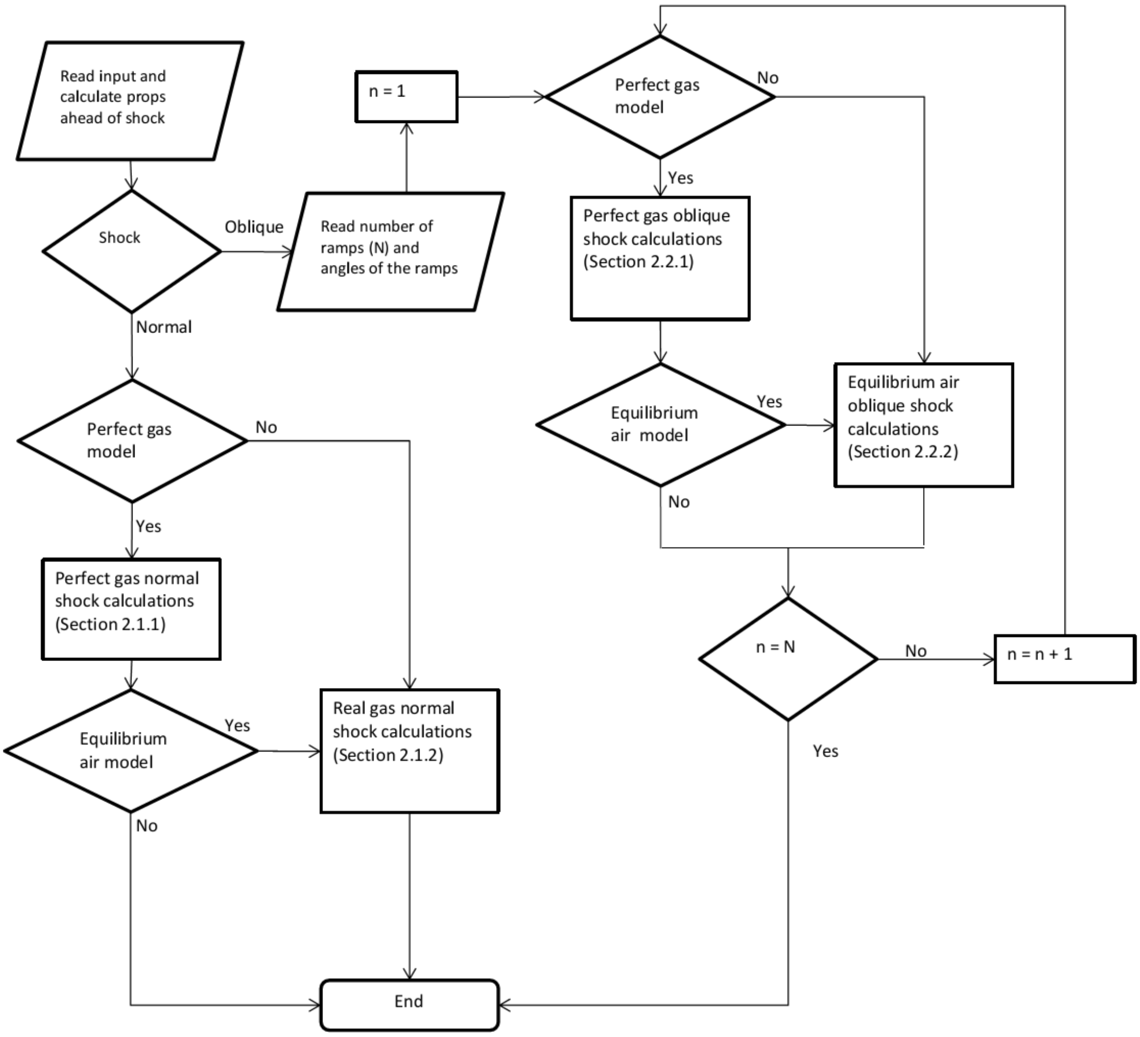


Figure 4 - Simplified Program flowchart.

## 3. MODEL VALIDATION AND PROGRAM VERIFICATION

Validation was made for both normal and oblique shock waves using results presented by Wittliff and Curtis (1961) and Nagamatsu *et al.*, 1959 and Anderson (1989), respectively. Table 1 presents atmospheric data used to validate the program normal shock wave calculations, with speeds ranging from 610 to 7925 m/s (2,000 to 26,000 ft/s), at altitudes of 15.24 and 30.48 km (50,000 and 100,000 ft).

Table 1 - Atmospheric parameters for normal shock wave validation taken from Wittliff and Curtis (1961)

| Altitude (km) | 15.24 | 30.48 |
|---|---|---|
| Pressure (Pa) | 11,664 | 1,105 |
| Temperature (K) | 217 | 233 |

Figure 5 - Temperature ratio across the normal shock wave as function of free stream speed at 15.24 km and 30.48 km altitude. models as well as the equilibrium ones obtained by Wittliff and Curtis (1961) as function of free stream airflow speeds. The calorically perfect gas model in the program has been exhaustively verified against results found in the literature. As can be seen in this figure, the program equilibrium gas model results compare quite well with the ones obtained in the above reference. Also, it can be noticed in this figure that high temperature effects get more important as the velocity and altitude (lower atmospheric pressure) increase, although the pressure is only slightly affected in basically the entire velocity range.

Temperature, as expected, is lower behind the shocks for equilibrium air in comparison with calorically perfect air. This is explained by the activation of the vibrational energy of the molecules and eventual dissociation, both consuming energy from the system and reducing its overall temperature.

ISSN 2176-5480



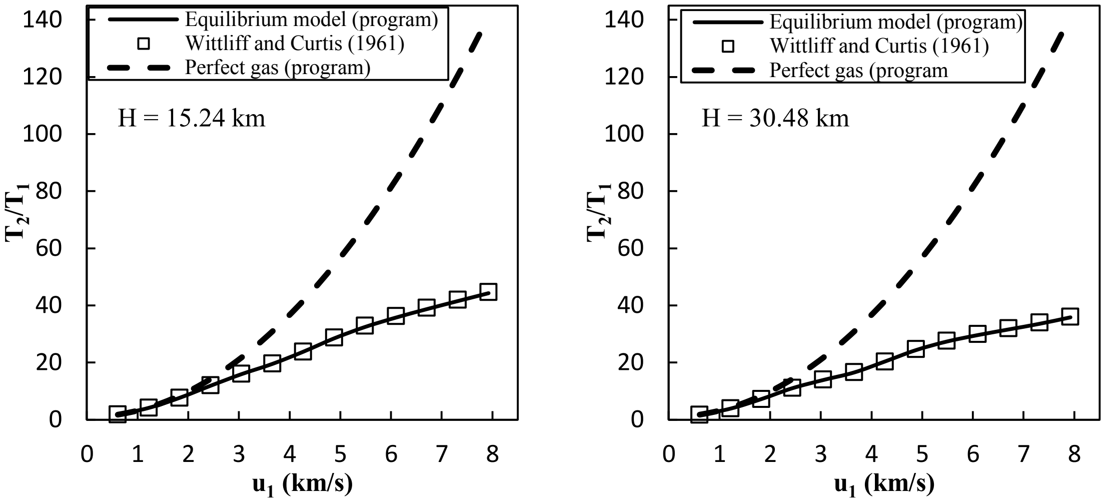


Figure 5 - Temperature ratio across the normal shock wave as function of free stream speed at 15.24 km and 30.48 km altitude.

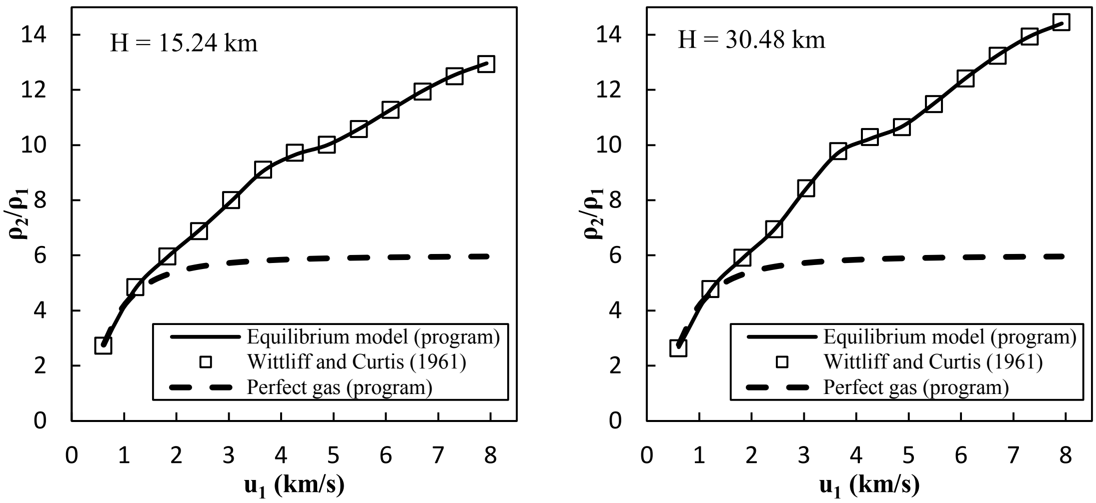


Figure 6 - Density ratio across the normal shock wave as function of free stream speed at 15.24 km and 30.48 km altitude.

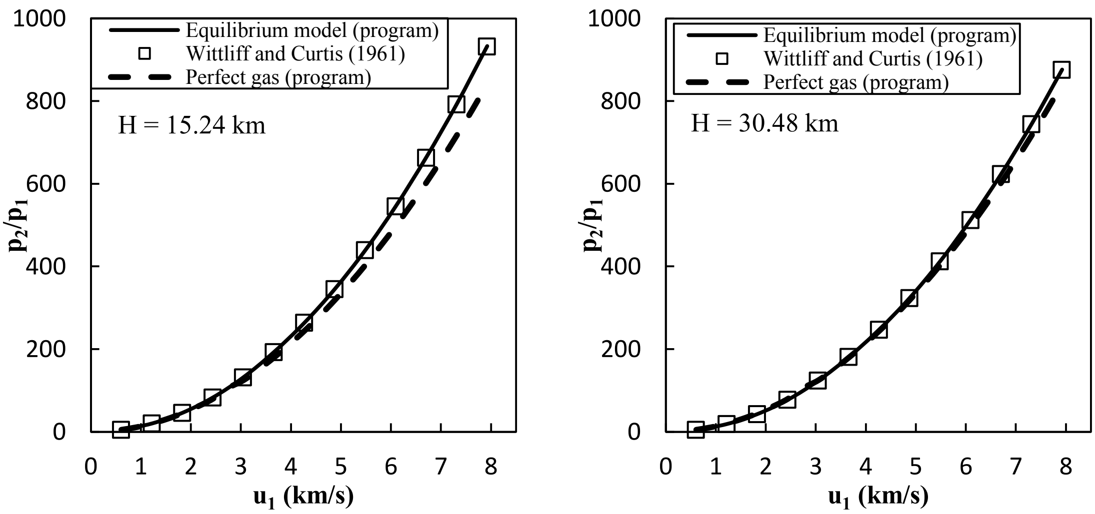


Figure 7 - Pressure ratio across the normal shock wave as function of free stream speed at 15.24 km and 30.48 km altitude.

ISSN 2176-5480



To validate the oblique shock wave calculations in the program, data was used from Nagamatsu (1959), with input values given in **Erro! Fonte de referência não encontrada.**, while varying the deflection angle *θ*. Data provided by Anderson (1989) was also used to further validate the calculation of the shock wave angle *β*. In the latter, three velocity values were chosen: (a) 1524 m/s (5000 ft), (b) 3048 m/s (10000 ft) and (c) 4572 m/s (15000 ft), considering an altitude of 30.48 km (100000 ft) and varying deflection angle *θ*.

.

Table 2 - Input values used for oblique shock wave validation, taken from Nagamatsu *et al.,*1959

| | |
|---|---|
| **Mach number** | 7.8 |
| **Temperature (K)** | 450 |
| **Pressure (Pa)** | 142 |

Figure 8 presents oblique shock wave angle results calculated with the program and the ones obtained by Nagamatsu *et al.*, 1959; and by Anderson (1989), for three different free stream speeds, at 30.48 km (100,000 ft) altitude as function of the deflection angle, $\theta$. As can be seen in this figure, the values calculated by the program correctly fit the values presented in both references.

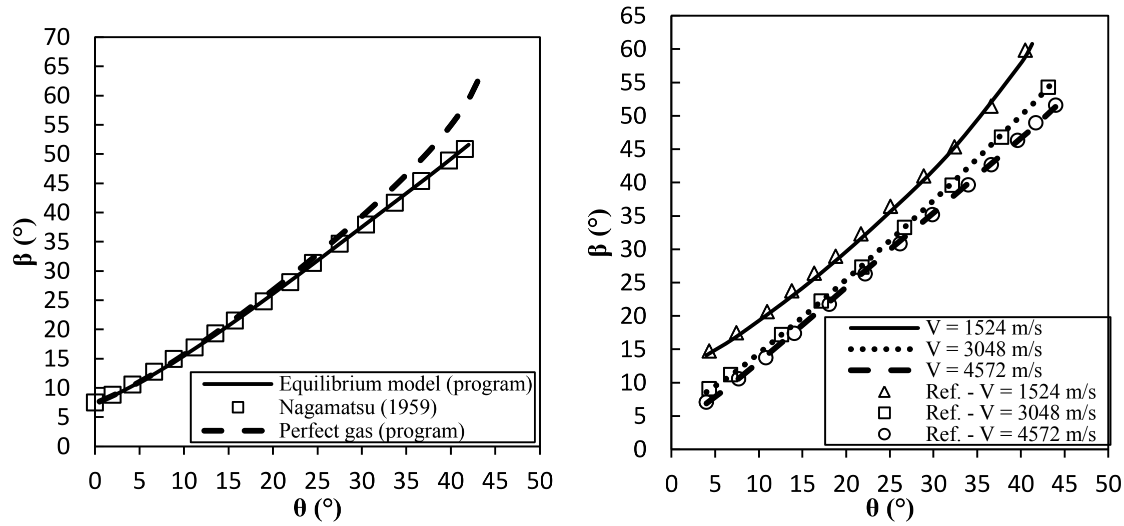


Figure 8 – Shock wave angle *β* as function of deflection angle *θ* calculated with the program and the ones obtained by Nagamatsu (1959) and Anderson (1989).

**Erro! Fonte de referência não encontrada.** Figure 9 **Erro! Fonte de referência não encontrada.**presents the temperature, density and pressure ratios across an oblique shock as a function of *β* in comparison with the ones obtained by Nagamatsu (1959). As can be observed in this figure, there is only a minor difference in basically all properties between the program and Nagamatsu's results. Anyway, it is believed the results of the program are more accurate because it uses the polynomial fits presented by Srinivasan *et al.*, 1987, which are more recent and elaborated than the ones used by Nagamatsu in 1959.

ISSN 2176-5480



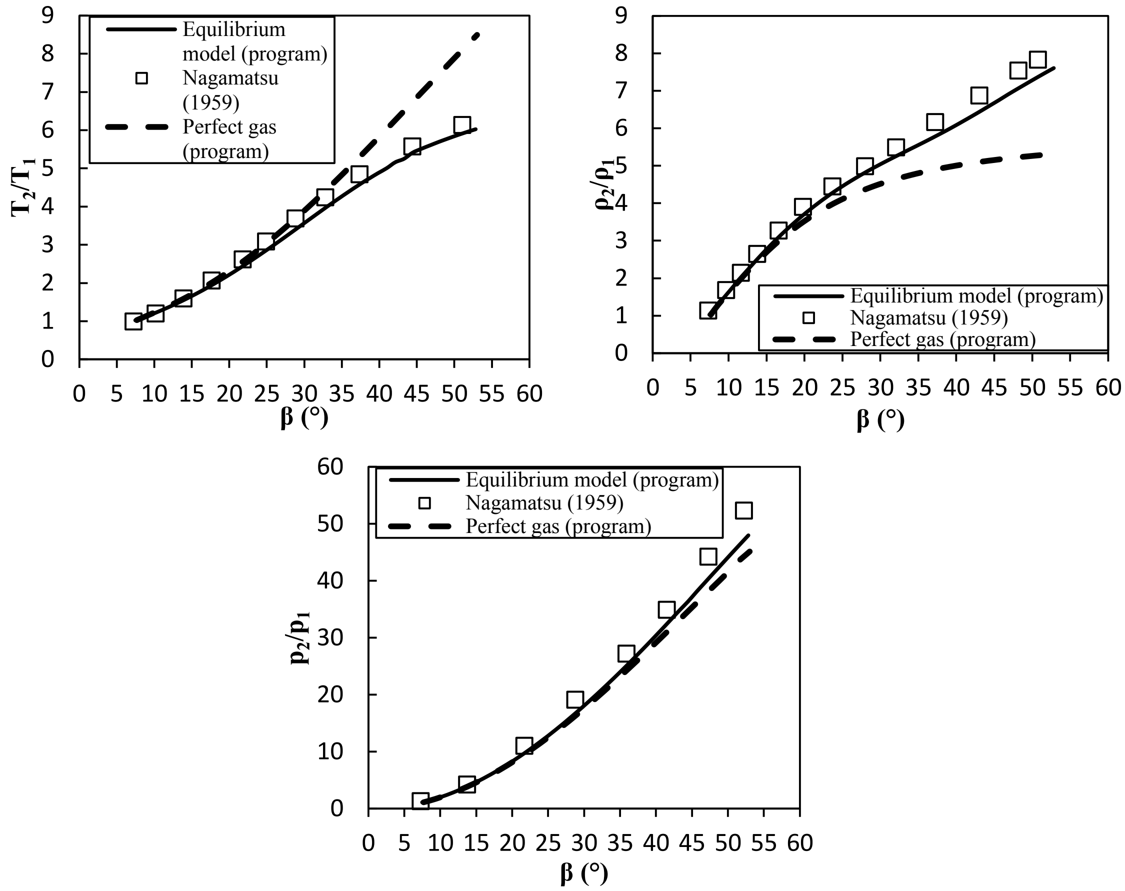


Figure 9 – Flow property ratios across oblique shocks with different wave angles calculated with the program and the ones obtained by Nagamatsu (1959).

## 4. SCRAMJET CALCULATIONS

The program has been used to calculate the airflow properties at the entrance of the isolator, which connects to the combustor, for the scramjet engine configuration being presently tested for the Brazilian 14-X airspace hypersonic vehicle under development at the Institute for Advanced Studies (IEAv). All calculations have been performed considering a series of ramps generating oblique shocks, with one last reflected shock right ahead of the isolator entrance, as shown schematically in Fig. 9, where the airflow properties have been determined. Results were obtained for free stream dynamic pressures of 25 kPa and 100 kPa, and speed ranging from 1500 m/s to 4000 m/s, which are closely practical limits for scramjet operation. Table 3 and Table 4 show, respectively, the free stream airflow data for the dynamic pressure of 25 kPa, and 100 kPa e.

Table 3 - Free stream airflow data for dynamic pressure of 25 kPa.

| | | | | | | |
|---|---|---|---|---|---|---|
| **H (m)** | 28780 | 32515 | 35365 | 37768 | 39854 | 41702 |
| **u (m/s)** | 1500 | 2000 | 2500 | 3000 | 3500 | 4000 |
| **p (Pa)** | 1409 | 804 | 530 | 377 | 283 | 256 |
| **T (K)** | 225,43 | 230 | 238 | 245 | 251 | 221 |
| **M** | 4,984028 | 6,577703 | 8,083155 | 9,565556 | 11,02902 | 13,43473 |

Table 4 – Free stream airflow data for dynamic pressure of 100 kPa.

| | | | | | | |
|---|---|---|---|---|---|---|
| **H (m)** | 20000 | 23600 | 26435,5 | 28780 | 30782 | 32515 |
| **u (m/s)** | 1500 | 2000 | 2500 | 3000 | 3500 | 4000 |
| **p (Pa)** | 5475 | 3118 | 2014 | 1409 | 1042 | 804 |
| **T (K)** | 216,65 | 220,25 | 223 | 225,43 | 227 | 230 |
| **M** | 5,084016 | 6,723061 | 8,350248 | 9,968055 | 11,5781 | 13,15541 |

Figure 10 illustrates the scramjet intake geometry used. The slashed lines represent shock waves generated by the ramps and $\theta$ are the flow deflection angles due to the ramps, which are presented in Table 5. As can be seen, the airflow at the isolator entrance has been subjected to the compression of three oblique shocks. For such a configuration, the program can be used, assuming a sequence of ramps, to calculate the airflow properties at the isolator entrance, which are approximately the conditions of the air entering the scramjet combustion chamber.

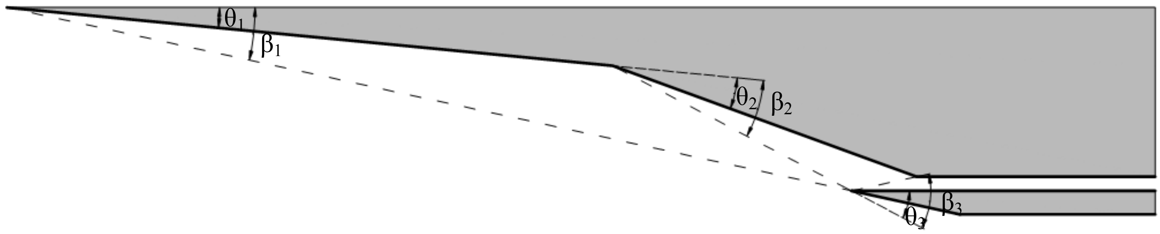


Figure 10 – Scramjet air intake geometry schematic.

Table 5 – Oblique shock deflection angles.

| Deflection angle (°) | Case 1 |
|---|---|
| **$\theta_1$** | 5.5 |
| **$\theta_2$** | 14.5 |
| **$\theta_3$** | 20 |

Figure 11 through Figure 13, present, respectively, the temperature, pressure and Mach number behind the last shock, i.e., at the isolator entrance, for both dynamic pressure values and gas models for the air.

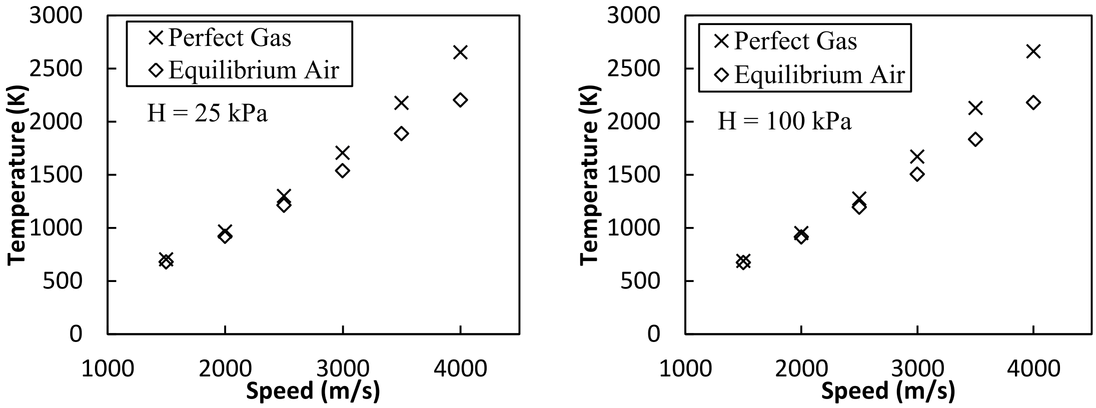


Figure 11 - Temperature at the isolator entrance considering air as both calorically perfect gas and in chemical and thermodynamic equilibrium, for dynamic pressure of 25 kPa and 100 kPa.

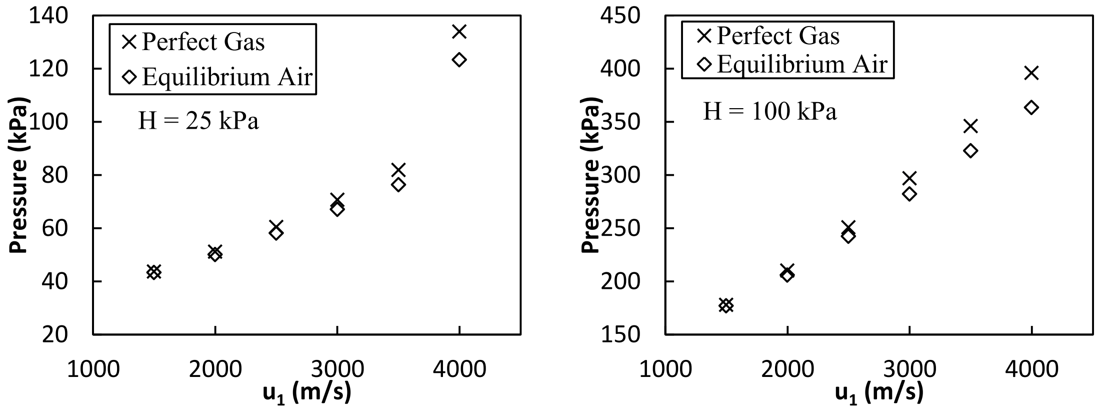


Figure 12 - Pressure at the isolator entrance considering air as both calorically perfect gas and in chemical and thermodynamic equilibrium, for dynamic pressure of 25 kPa and 100 kPa.

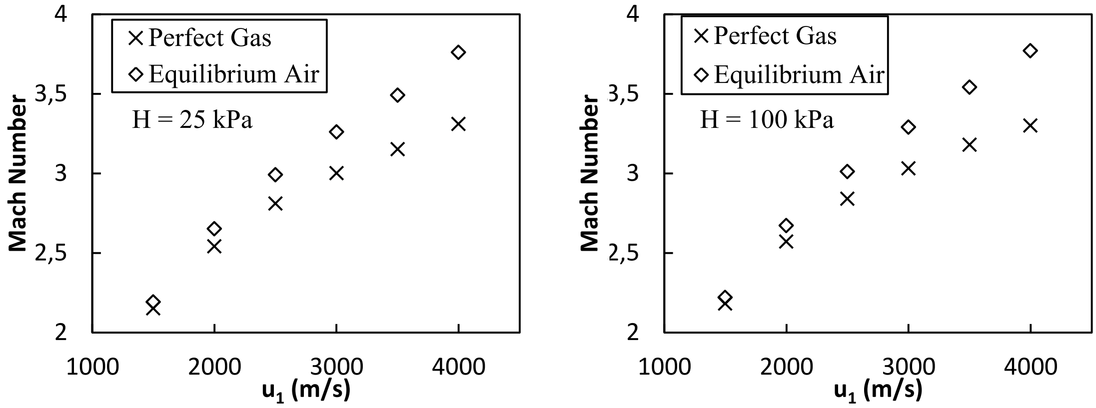


Figure 13 – Mach number at the isolator entrance considering air as both calorically perfect gas and in chemical and thermodynamic equilibrium, for dynamic pressure of 25 kPa and 100 kPa.

As expected, the results show that high temperature effects on the air in scramjets become important only at considerably high speeds, let say, above 3,000 m/s. As can be seen in Fig. 11, the calculated temperature with the more accurate equilibrium gas model is about 500 K below the calorically perfect gas value at about 4,000 m/s. Consequently, Mach number is also considerably affected mainly because of the change in the sound speed calculated by both models. On the other hand, pressure is not much affected even at high speeds and, differently from what have been observed for normal shocks, the pressure is lower for the equilibrium air model. This is because the shock wave angles are smaller for equilibrium air, resulting in a less intense shock and, therefore, lower pressure ratios across the oblique shock waves.

## 5. COMMENTS AND CONCLUSIONS

In order to facilitate the project of a scramjet engine, a computer program was newly developed to allow for easier calculations of properties across both normal and oblique shocks, the latter possible for a sequence of several ramps. The program was created to make calculations for both air as a calorically perfect gas and for chemical and thermodynamic equilibrium.

Results were generated for program verification and validation of the model, in comparison with results from the literature. Also, scramjet inlet results were obtained for air in both chemical and thermodynamic equilibrium and as perfect gas. The results obtained showed good correlation with the literature for both normal and oblique shock waves, validating the use of the program for the proposed applications. The obtained results for the scramjet inlet show the effects of chemical and thermodynamic equilibrium air, with temperatures lower than those for perfect gas, generating a less intense shock wave.

The program is user-friendly and performs quick calculations of the properties across shock waves, saving time on calculations necessary during the project activities.

## 6. ACKNOWLEDGMENTS

This work has been performed with CNPq/AEB financial support under the Project number 560143/2010-9.

## 7. REFERENCES

Anderson, J. D., 1989. *Hypersonics and High Temperature Gas Dynamics*. McGraw-Hill, New York.

Anderson, J. D., 1990. *Modern Compressible Flow*. McGraw-Hill, New York, 2$^{nd}$ edition.

Tannehill, J. C. and Mugge, P. H., 1974. "Improved Curve Fits for the Thermodynamic Properties of Equilibrium Air Suitable For Numerical Computation Using Time-Dependent or Shock-Capturing Methods".

Srinivasan, S., Tannehill, J. C. and Weilmuenster, K. J., 1987. "Simplified Curve Fits for the Thermodynamic Properties of Equilibrium Air".

Wittliff, C. and Curtis, J., 1961. "Normal shock wave parameters in equilibrium air". Buffalo, NY

Nagamatsu, H. T., Workman, J. B. & Sheer Jr., R. E., 1959, "Oblique shock relations for air at Mach number 7.8 and 7200$^{o}$R stagnation temperature". New York, NY

## 8. RESPONSIBILITY NOTICE

The authors are the only responsibles for the printed material included in this paper.